Table-Based Dynamic PHEMT Model Using Delayed Capacitive Currents

C. J. Wei, A. Klimashov, J. Gering and Y. Tkachenko

SKYWORKS SOLUTIONS INC. 20 Sylvan Road, Woburn, MA 01801,USA.
Phone:+781-3763214, Email: Ce-Jun.Wei@skyworksinc.com

***Abstract* — A new table-based large-signal FET model using delayed capacitive currents is developed to account for nonquasi-static features of PHEMTs at high frequency. Unlike conventional models, it does not contain real charge terms and only utilizes capacitance currents and therefore, avoids the problem of path-dependence in the charge-integration based on small-signal models. Consideration is also given to the HF dispersion of conductances. It is found that frequency-dependence of conductances is responsible for the deviation in fitting S-parameters at high frequency. Bias-dependent delay times associated with capacitance terms are included in the model. The model features accuracy and simplicity of extraction. It is especially useful for high frequency PHEMTs or FETs with dispersion.**

I. INTRODUCTION

A large variety of Large-signal FET/PHEMT empirical and table-based models have been developed and now are commercially available. High accuracy has been achieved for those devices that satisfy charge conservation and show insignificant dispersion [1-11]. However, an industry standard model is still lacking and there are problems that require more dedicated efforts to resolve.

The major difficulty is that conventional large-signal models that fit DC IV and QV characteristics are often inconsistent with small-signal models. Small-signal models have no charge terms but capacitance terms. A small-signal model, on the other hand, derived from a conventional large-signal model contains as many as four trans-capacitance elements that makes the consistency very difficult. Also small-signal models have no current but conductance terms. The currents and charges in large-signal model obtained from integration of measured small-signal element values are normally not unique because of the integration path-dependence due to dispersion. The other problem applies to HF response. Conventional Π-shaped equivalent circuit becomes too simple to fit the HF response. The element values of small-signal models become frequency-dependent.

The new model proposed here, has several distinct features. (1) It does not contain charge terms and the currents caused by the time-variance of charges are replaced with capacitive currents [8]. (2) RF conductance and RF-trans-conductance values are different from those at DC which is accounted for by using feedback and feed-forward circuit. (3) Major HF-frequency-dependent elements are the terms related to dispersion of conductance, which can be represented by time-delayed capacitance currents [10]. (4) The nonlinear functions are all table-based and extracted from the bias-dependent small-signal model values. The first three features ensure complete consistency with conventional small-signal models, since they have an exact correspondence between the model elements. In the new model there is no ambiguity involved because there are no trans-capacitance terms, except for one that translates to a delay time in connection with Gm. The fourth feature avoids complex and tedious fitting or optimization and makes the model technology-independent [2].

II. EQUIVALENT CIRCUIT MODEL

The currents flowing in a nonlinear device can be represented in time domain by:

$$\mathbf{I} = f(I, \partial/\partial t, \partial^2/\partial t^2, \ldots.)\ \mathbf{V}$$

where **I, V** are (ig, id) and (vg, vd) vectors. Developing the f into linear term of derivatives and neglecting high-order terms, we have:

$$\mathbf{I} = fo(\mathbf{V}) + \partial\,\mathbf{Q(V)}/\partial t + \partial^2\,\mathbf{U(V)}/\partial t^2 \ldots.$$
$$= fo(\mathbf{V}) + C(\mathbf{V})\,\partial\mathbf{V}/\partial t + D(\mathbf{V})\,\partial^2\mathbf{V}/\partial t^2$$

The first and second terms are DC current and capacitive current, respectively. The third term can be translated as frequency dependent parts of the conductances, when we convert to frequency domain and take the small-signal part.

$$\mathbf{i} = g\mathbf{V} + j\,\omega C\,\mathbf{V} - \omega^2 D\mathbf{V} \ldots.$$

The third term can also be expressed as a time delayed capacitive current, providing that the delay-time is small.

$$\mathbf{I} = fo(\mathbf{V}) + \partial Q(\mathbf{V(t-\tau)})/\partial t$$
$$= fo(\mathbf{V}) + C(\mathbf{V})\,\partial\mathbf{V}/\partial t - \partial(\tau\, C(\mathbf{V})\,\partial\mathbf{V}/\partial t)/\partial t$$

Providing that C(**V**) is a slow function of **V**, we obtain $D = -\tau\mathbf{C}$.

For the first two terms, the current flowing into branch i, is divided into two classes of currents: conductive currents, such as drain/gate current, and capacitive currents $C_{ij}dv_j/dt$, where i=j are local terms and i≠j are non-local terms, and v_j is the RF voltage across the j-th branch. To separate the DC V_{jo} from the instantaneous Vi

and to create a voltage node dv_j/dt, the sub-circuits with large-RC constants shown in the left part of Figure 1 are used. We denote Vg and Vd as instantaneous gate and drain voltages, and Vgo and Vdo as their DC components.

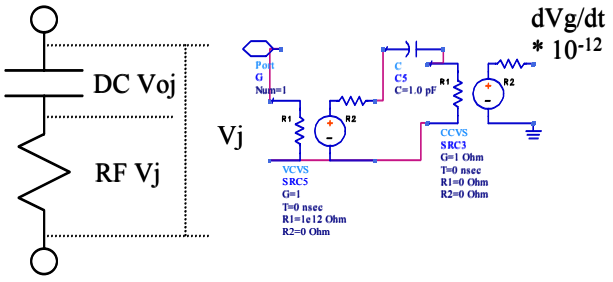

Figure 1. Sub-circuits to obtain DC Vjo, RF Vj and dVg/dt.

For the time-delay-related currents, we represent them as virtual charge terms $\mathbf{Q}=-\tau C(\mathbf{V})\partial\mathbf{V}/\partial t$. The associated currents are $-\partial(\tau C(\mathbf{V})\,\partial\mathbf{V}/\partial t)/\,\partial t$.

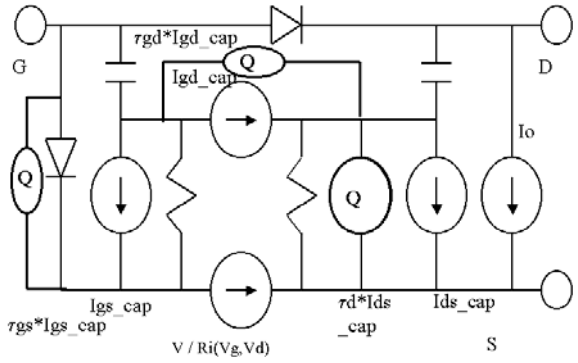

Figure 2. Intrinsic nonlinear currents of the model

Figure 2 shows the intrinsic part of the device model. The zero DC component of capacitive current is assured by using series RC circuits with RC>>1/f and R>1 MOhm. The dVj/dt is obtained as shown in the right part of Figure 1. The voltage Vj is applied across the 1pF capacitor, and the current through the capacitor is equal to dVj/dt multiplied by the factor of 1e-12. Here, we use 1pF instead of a 1F to reduce the numerical error at high frequencies. The capacitive current is simply the product of nonlinear function of C(**V**) and node d**V**/dt.

The currents are expressed as:

$$\text{Ids\_cap1}= \text{Cm}(\text{Vg},\text{Vd})\cdot d\text{Vgs}/dt$$
$$\text{Ids\_cap2}= \text{Cds}(\text{Vg},\text{Vd})\cdot d\text{Vds}/dt$$
$$\text{Igd\_cap}=\text{Cgd}(\text{Vg},\text{Vd})\cdot d\text{Vgd}/dt$$
$$\text{Igs\_cap}=\text{Cgs}(\text{Vg},\text{Vd})\cdot d\text{Vgs}/dt$$

where Ids_cap, Igd_cap and Igs_cap are the capacitive currents flowing through branches D-S, D-G and G-S, respectively, and Cm=-Gm·tau. There is an additional current from internal node at the gate-end of the channel to the source that accounts for the nonlinear channel resistance Ri.

In the new model, three additional charge terms associated with respective capacitive currents are used with bias-dependent time constants, τg, τgd, τd and τm. Assuming a small deviation of the port voltages and neglecting the higher-order terms, one finds that the currents have the following correspondence to the elements of the small-signal model:

$$\text{Igs\_cap}\Rightarrow\text{Cgs}$$
$$\text{Igd\_cap}\Rightarrow\text{Cgd}$$
$$\text{Ids\_cap}\Rightarrow-\text{Gm}\cdot\tau+\text{Cds}$$
$$\text{Irf1}\Rightarrow\text{Gm},\ \text{Irf2}\Rightarrow\text{Gds}$$
$$\partial(\tau d\ \text{Ids\_cap2}/\partial t)\Rightarrow\omega^2\text{ part of Gds}$$
$$\partial(\tau g\text{Igs\_cap}/\partial t)\Rightarrow\omega^2\text{ part of Ggs}$$

The dispersion of RF conductances with respect to DC at bias point is achieved by the feed-back and feed-forward circuits with coefficients cbk and cfw, to account for the difference between Gds|rf and Gds|dc and between Gm|rf and Gm|dc:

$$\text{Gm|rf}=\text{Gm|dc}\ (1+\text{cfw})$$
$$\text{Gds|rf}=\text{Gds|dc}\ (1+\text{cbk})$$

The model elegantly shows one-by-one correspondence of large-signal elements to small-signal elements leading to complete consistency. Moreover, the charge terms are replaced with capacitive currents, making the model extraction much easier and faster.

III. MODEL EXTRACTION AND IMPLEMENTATION

The model extraction starts with "Cold FET" process to extract the parasitic resistances and inductances. The intrinsic elements of the small-signal models are extracted at lower frequencies and at hundreds of bias points from the cutoff region to the active region, typically Vg from –3 V to forward bias, and Vds from 0 to 7.5 V. The extraction of intrinsic elements is also performed at higher frequency end. By comparing the difference of GS, GD and DS conductances extracted at HF and at low frequencies, we can extract the time constants, τgs, τgd, and τd:

$$\tau gd =(\text{Re}(Y12h)-\text{Re}(Y12l))/(\text{Cgd}\ (\omega_h^2-\omega_l^2))$$
$$\tau d=(\text{Re}(Y22h)+\text{Re}(Y12h)-\text{Re}(Y22l)-\text{Re}(Y12l))/(\text{Cds}\ (\omega_h^2-\omega_l^2))$$

Assuming charge conservation holds, we have:

$$\tau gd=\tau g$$
$$\tau m=\tau d-\tau dg$$

Index h specifies high frequency and l specifies low frequency. The Y parameters refer to the intrinsic admittance matrix after de-embedding the parasitics

Table-based model was implemented with a symbolic-defined device (SDD) in ADS2001. A general MDIF file is generated for access the bias-dependent data-table for current, capacitances, feed-through coefficients and time-constants. In the model, the current and capacitances read as instantaneous values whereas the feed-through coefficients and time-constants read as

values at bias-point only. Self-heating effects are also included in the model by using the thermal sub-circuit.

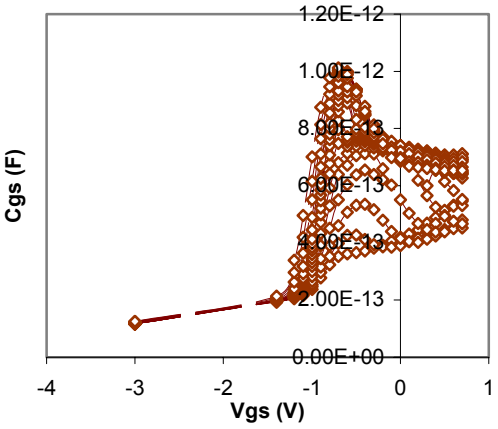

Figure 3. Fitted (lines) and measured (symbols) Cgs as a function of Vgs with Vds as a parameter.

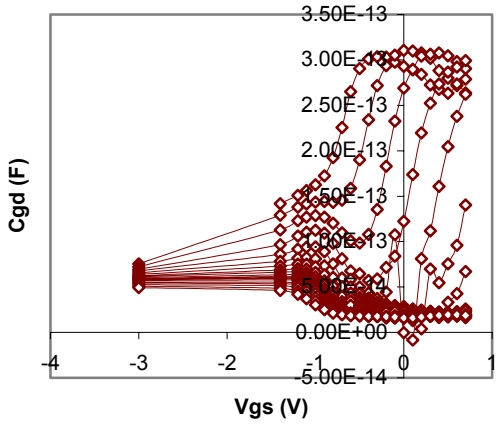

Figure 4. Fitted (lines) and measured (symbols) Cgd as a function of Vgs with Vds as a parameter.

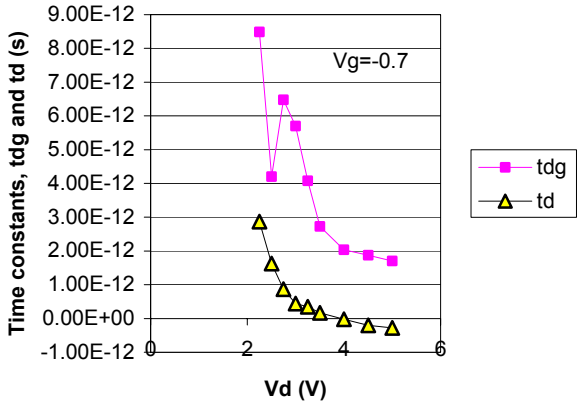

Figure 5. Fitted (line) and measured (symbol) tgd and td as a function of Vds with Vgs=-0.7V.

V. MODEL VALIDATION

The model was verified by simulation of small-signal response, large-signal power and two-tone inter-modulation distortion characteristics of Skyworks PHEMT and MESFET devices. The small-signal models are extracted for a wide range of biases with Vgs varying from -3 to 0.6 V and Vds varying from 0.25 V to 7.5 V using an in-house program. During simulation table-formatted large-signal relations are interpolated using standard spline routine available in ADS. Figure 6 shows the modeled and measured S-parameters up to the cutoff frequency for the 0.25um gate length 6x200 um PHEMT device at Vg=-0.7 V, Vd=4 V. The fitting at other bias points has also been verified.

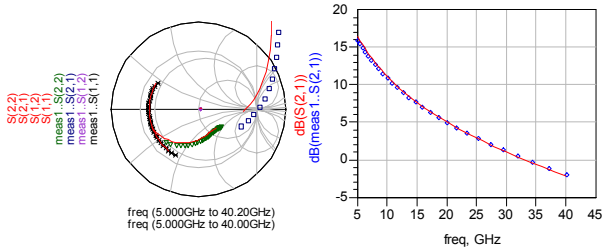

Figure 6. Modeled (line) versus measured (symbol) S11, S22, S12, and S21 at a typical operating bias point.

Figure 7 shows the modeled and measured power performance of this device at f = 5.8 GHz, source Gamma of 0.69∠131.3, and load Gamma = 0.04∠1.1. The device is biased at Vgs = -0.7 V and Vds = 3 V. Very good agreement is achieved between the modeled and measured data.

To further validate the accuracy of the model with respect to inter-modulation distortion characteristics, we used a 6x200 um MESFET and measured the two-tone performance at 1.8GHz. The load reflection coefficients presented to the device on the load-pull station were: 0.28∠123 at the fundamental, 0.9∠8.6 at the second harmonic, 0.533∠168 at the third harmonic. The source reflection coefficients presented to the device were: 0.35∠104.5 at the fundamental and 0.61∠-51 at the second harmonic. The spacing between the tones was 1 MHz.

Figure 8 compares the simulated and the measured third and fifth order inter-modulation products. It shows very good agreement, except for the low power region where the simulated fifth order IMD is higher than the measured. Since the table-based model uses only cubic spline functions for interpolation, for the smaller RF swing at low power which is comparable to the grid spacing, function derivatives higher than third order vanish leading to inaccuracy in two-tone simulation.

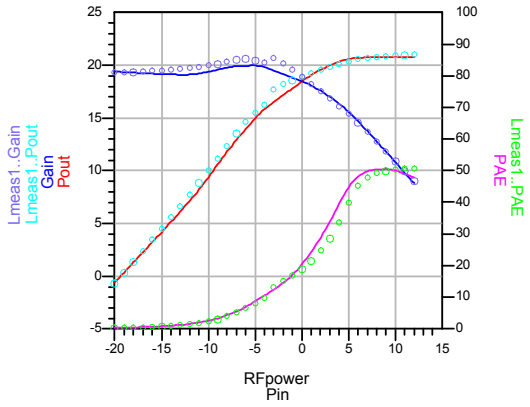

Figure 7. Simulated (line) vs measured (symbol) power performance of a 10x50 um PHEMT at f = 5.8 GHz, Vgs = -0.7 V and Vds = 3V.

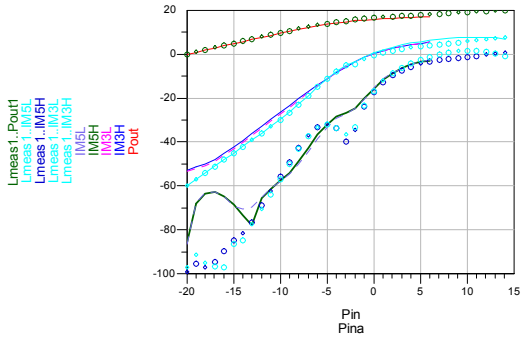

Figure 8. Simulated (line) vs measured (symbol) two-tone performance of a 6x200 um MESFET at f = 1.8 GHz, Vgs=-1 V and Vds = 3V.

VI. Conclusion

A new table-based large-signal MESFET/PHEMT model is developed. The new model is based on the one-for-one correspondence between the small-signal model elements and nonlinear functions of port voltages and therefore features consistency between the large-signal and small-signal models. The DC/RF dispersion effects can be effectively handled by using feed-through circuits and the HF dispersion was accounted for by the use of charge time delay constants. The model is accurate to near cutoff frequency, yet calculation-efficient. It is more complex and yet simple to extract. In addition to small-signal characteristics, the model is validated using power, power-added efficiency and two-tone inter-modulation distortion characteristics.

References

[1] W. Curtice, M.Ettenberg, "A nonlinear GaAs FET model for use in design of output circuit of power amplifiers," *IEEE Trans Microwave Theory & Tech,* vol.33, no.12,pp1383,1985

[2] D. E. Root, S, Fan, and J. Meyer, "Technology-independent Large-signal FET Model: A measurement-based Approach to Active Device Modeling," 1991, *Proc. 15th ARMMS Conference*

[3] I. Angelov, "Chalmers Nonlinear HEMT and MESFET model," *Report 26, Chalmers University of Technology*, ISSN 1103-4599

[4] C. J. Wei, Y. A. Tkachenko, and D. Bartle, "An accurate large-signal model of GaAs MESFET which accounts for charge conservation, dispersion, and self-heating," *IEEE Trans Microwave Theory & Tech,* vol.11, pp.1638-, 1998

[5] C. J. Wei, Y. A. Tkachenko, and D. Bartle, "A new analytic model for power E-mode PHEMTs and its optimum power operation," presented at IMOC'99, Rio-de-Janeiro, Aug.9-12, 1999.

[6] Ph. Jansen, D. Schreurs, W. De Raedt, B. Nauwelaers, and M. Van Rossum, "Consistent small-signal and large-signal extraction techniques for heterojunction FETs," in IEEE Trans. on Microwave Theory and Tech., Vol. 43, No. 1, Jan. 1995, pp. 87-93.

[7] C. J. Wei, J. Gering, Y. A. Tkachenko and D. Bartle, "Completely Consistent 'No-Charge' PHEMT Model Iincluding DC/RF Dispersion," *Digest, 2002 International Microwave Symposium*, pp.2137-2141, Seattle, 2002

[8] M. C. Filicori and G. Vannini, "Mathematical Approach to Large-signal Modeling of Elecronic Devives," 1991, *Electronic Devices*, Vol.27, pp.357-359

[9] M. F-Barciela, P. J. Tasker, Y C-Roca, M. Demmler, H. Massler, M. C. C-Francos, and M. Schlechtweg, "A simplified Broad-Band Large-Signal Nonquasi-Static Table-Based FET model," *IEEE Tran. Microwave Theory andtechnique* , vol. 48, no.3, pp.395-403, 2000

[10] V.I. Cojocaru and T.J. Brazil, "A Scalable General-Purpose Model for Microwave FET's Including the DC/AC Dispersion Effects,", IEEE Trans. On MTT, Vol.45, No.12, 1997

[11] C.-J. Wei, Y.A. Tkachenko and D. Bartle, "Alpha Owned PHEMT Model and Its Verification by Load-Pull and Waveform Measurements," 2000-APMC, Sydney, Australia, Dec.2-6, 2000